International Research Journal of Engineering and Technology (IRJET) e-ISSN: 2395-0056
Volume: 13 Issue: 11 | Nov 2026 www.irjet.net p-ISSN: 2395-0072

ENHANCED OPTOMECHANICAL TRANSDUCTION OF LARGE AMPLITUDES THROUGH RACETRACK-LOADED MACH–ZEHNDER INTERFEROMETERS

SURABHI GUPTA[1]

[1]*Assistant Prof., Department of Applied Sciences and Humanities (Engineering Physics), VSGOI, Unnao, AKTU, U.P India*

Abstract:-*On-chip integrated photonic devices have driven advances in fields ranging from telecommunications to optomechanics. Racetrack resonators have become popular for optomechanical transduction due to their high sensitivity and high cavity finesse. However, they lack a sufficient dynamic range to allow for the readout of large-amplitude mechanical resonators, which are preferred for sensing applications. We present a robust photonic circuit, based on a Mach-Zehnder interferometer (MZI) combined with a racetrack resonator, that increases the linear range without compromising transduction sensitivity. The optical and mechanical properties of these combined devices (MZI-resonator) are compared to those of isolated resonators with the same physical dimensions, across weak, strong, and critical coupling regimes. We demonstrate an overall improvement in dynamic range, transduction response, and mass sensitivity, with enhancement factors of 4, 3, and 2.8, respectively. Our MZI circuit, which features high phase sensitivity, also paves the way for applications such as on-chip integrated homodyne optical sensing.*

INTRODUCTION

In recent years, silicon-based photonic devices such as modulators and resonators, originally designed for telecommunications have been repurposed as ultrasensitive optical detectors for mass or temperature [1–4], as well as for the on-chip transduction of mechanical motion [5,6]. Easier access to photonic integrated circuit (PIC) fabrication facilities has made integrated photonics a versatile and cost-effective option for designing highly responsive optomechanical devices. Efforts to develop on-chip optomechanics as a sensing platform have primarily focused on optimizing the quality factor (Q) both optical and mechanical and reducing the mechanical modal mass [5]. Conversely, little attention has been paid to the role that the linearity range of an optical cavity plays in mitigating readout nonlinearities during mechanical transduction [7]. Optomechanical crystals, microring resonators [8,9], and ring-shaped resonators have been consistently explored as sensing elements characterized by a high Q-factor and high cavity finesse; this enables exceptional displacement sensitivity and high signal-to-noise ratios [5,6,10]. However, the narrow linewidth of these cavities inherently precludes the linear transduction of large-amplitude mechanical modes (i.e., it limits the dynamic range). Furthermore, it renders the optomechanical system sensitive to environmental perturbations such as gas adsorption or temperature fluctuations which cause shifts in the cavity's resonance wavelength [1,2,11]. The resulting variation in cavity detuning can introduce significant readout nonlinearities or even lead to the loss of the mechanical signal [12]. Furthermore, current approaches aimed at enhancing nanomechanical sensitivity by reducing modal mass are bolstered by increased optomechanical coupling [5]. This inevitably leads to stronger coupling and larger amplitudes and they induce nonlinearities in the nanomechanical readout, which impairs sensor performance [7,12,13]. In general, large-amplitude vibrations associated with a linear readout are desirable to maximize the dynamic range in optomechanical sensing [1,14–16] particularly for the measurement of mass [1,2,11], temperature [3,4,11], and force [17] in fluid or atmospheric environments characterized by a low quality factor (Q) [1,11]. In this work, we present a robust photonic circuit design based on a Mach-Zehnder interferometer (MZI) [4,18–20] combined with a "racetrack" resonator a configuration referred to as an MZI coupled to a racetrack resonator which extends the linear range without compromising the high sensitivity of the optomechanical transduction. The devices are fabricated on a standard 220 nm silicon-on-insulator (SOI) substrate, which features a 2-micrometer buried oxide layer. We compare the optical resonance properties of 24 MZI-coupled racetrack resonator devices with those of 24 isolated racetrack resonators having the same physical dimensions across the overcoupled, undercoupled, and critically coupled regimes. The MZI-coupled racetrack resonators outperform the isolated racetrack resonators in terms of optical linear range: by a factor of 2 to 3 in the overcoupled regime, 1.8 times near critical coupling, and 3.2 times in the undercoupled regime. Furthermore, the sensitivity of photonic transduction improves by a factor of 1.7 to 3.5 in the overcoupled regime, while remaining comparable to that of an isolated loop-resonator architecture in the

undercoupled and critically coupled regimes. The improvements achieved over a design based solely on a loop resonator are validated by reading out the first (1f) and second (2f) harmonics of laterally coupled microcantilevers [5,6,13]. As evidenced by the emergence of the 2f signal, Mach-Zehnder interferometers (MZIs) coupled to a loop resonator provide an extension of the mechanical linear range by a factor of 3 to 4 in the undercoupled or critically coupled regimes, compared to reference loop resonators paired with microcantilevers of identical dimensions. This expansion of the linear range, enabled by the MZI, results in a 2.8-fold improvement in mass sensitivity, thereby paving the way for mass detectors with a wide dynamic range. Although cavity-based transduction of linear mechanical spectra can be extended to larger amplitudes, the range of linear proportionality between the mechanical amplitude and the overall signal power remains comparable. Since a Mach-Zehnder interferometer (MZI) circuit is, by nature, an extremely phase-sensitive device allowing for the conversion of phase measurements into amplitude measurements (and vice versa) it offers greater flexibility for applications such as on-chiphomodyne detection of mechanical signals [21–23].

THEORY:-

The response of a "racetrack" ring cavity exhibits variations in both amplitude and phase as a function of the cavity detuning. In conventional optomechanical transduction devices, the signal corresponding to mechanical motion for a given detuning is extracted either directly via modulation of the optical power within the cavity, or through phase-sensitive optical homodyne detection performed off-chip. A simple, on-chip integrable method for converting a phase signal into an amplitude signal involves coupling the ring cavity to one of the arms of a Mach-Zehnder interferometer (MZI). Direct access to the cavity's phase spectrum, following the mixing of the signals at the output, enables on-chip optical homodyne detection; furthermore, this approach offers an intrinsically larger linewidth compared to the amplitude spectrum for mechanical transduction. This mechanism is expected to extend the linear transduction range while preserving sensitivity (or "responsivity"). We have designed a nanophotonic circuit based on a Mach-Zehnder interferometer (MZI), consisting of a 50:50 input splitter, a reference arm that introduces a phase shift θ, and an arm that incorporates an "all-pass" racetrack ring resonator [7, 18, 19]. Figure 1 shows optical microscopy images of an MZI with an integrated on-chip ring cavity (a), as well as an isolated ring cavity (b); both devices feature identical dimensions and coupling conditions. For this device, which exhibits very high phase sensitivity, transfer functions are used to describe the path of the input light signal: through the reference arm, with , HREF(θ) = 1/,2 sieiθ , and the all-pass race track resonatorarm, HRT(φ).and through the arm containing the ring resonator, with ,HRT(φ).The phase shift accumulated during one complete round trip within the ring cavity can be approximated as follows:

$$\phi(x) = \frac{2\pi(\lambda - \lambda_{res}(x))}{\mathcal{F}} = \frac{2\pi}{\mathcal{F}}\left(\lambda - \frac{2\pi c\lambda_{res}}{2\pi c + Gx\lambda_{res}}\right) \quad (1)$$

where = λ2 LCng is the free spectral range, ng is the group index, LC is the cavity length, λ is the measurement wavelength, and λres(x) is the racetrack resonant wavelength. Recombination of the reference and signal fields at the output splitter produces a net amplitude sf given by the sum of the transfer functions. The transmitted field power of the racetrack-loaded MZI and bare.

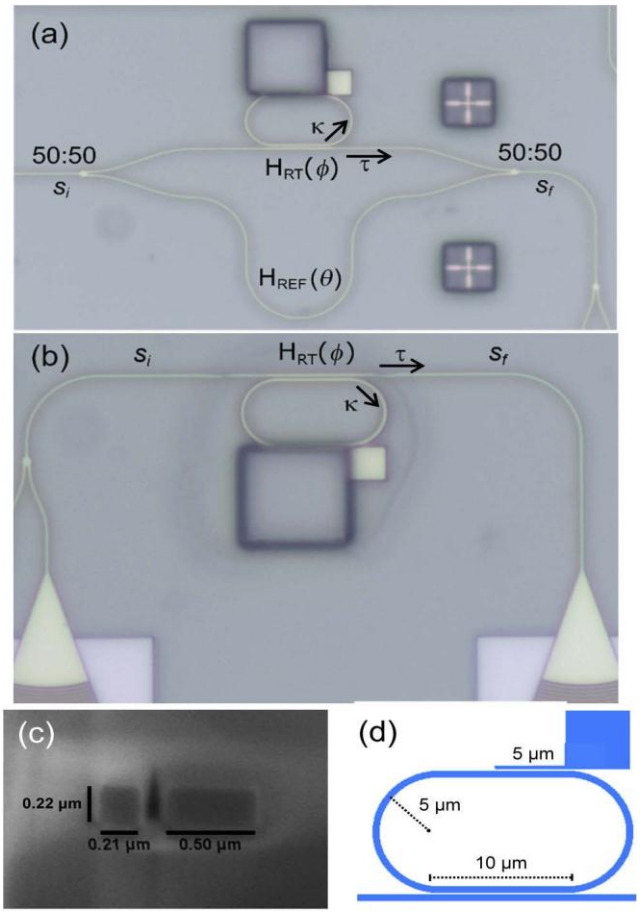

Fig. 1. Optical microscopy images of (a) a Mach-Zehnder interferometer (MZI) coupled to a racetrack resonator and (b) a racetrack resonator alone; both structures feature radii of 5 μm, straight sections of 10 μm, and laterally coupled mechanical arms (cantilevers) with a length of 5 μm.

The transfer functions HREF and HRTare shown in the graph, along with the transmission coefficient are depicted on-plot together with the transmission coefficient, τ, coupling coefficient, κ, and the phase shift, θ, of the 33 μm referencearm (Larm) to illustrate the phase tracking process. The incident light field si is split equally (50:50) between the two arms and subsequently recombined at a second 50:50 coupler to generate the output signal sf.. The dark square area visible next to the racetrack resonator in both images corresponds to an etch window used to release the narrow mechanical arm, which is anchored at one end and positioned parallel to the resonator. Only the anchor point of the mechanical arm appears as a light-colored square. Image (c), obtained via scanning electron microscopy, shows a cross-section prepared using a focused ion beam (FIB); it reveals a 210 nm-wide nanomechanical arm coupled to a 500 nm-wide racetrack waveguide, with a 160 nm gap and an active layer thickness of 220 nm. Panel (d) presents an in-plane schematic of the optomechanical system, consisting of the racetrack resonator and the mechanical arm.

EXPERIMENTAL DETAILS AND RESULTS

Mach-Zehnder interferometers (MZIs) integrating "racetrack" ring resonators as well as isolated ring resonators (used as references) with identical coupling conditions were fabricated on-chip at the AMF (formerly IME) foundry in Singapore. To tune the linear range and the slope of the resonance, four different coupling conditions were employed, with mean τ values of 0.923, 0.975, 0.986, and 0.994, corresponding to optical quality factors for the resonators ranging from 3,000 to 45,000. In each circuit, nanomechanical levers were integrated, coupled laterally near the straight section of the resonator. These levers had lengths of 2 μm, 3.5 μm, and 5 μm, with corresponding widths of 200 nm, 180 nm, and 180 nm; the gap between the lever and the resonator was either 160 nm or 200 nm. In total, 24 ring resonators and 24 MZI devices incorporating such resonators were fabricated. To characterize our circuits from both an optical and a mechanical perspective we used a confocal nanophotonic "pump-probe" measurement method, as described in references [5, 7, 26].

Optical characterization

The optical transmission spectra of the 24 racetrack-loaded MZIs and 24 reference racetracks were measured using a Santec TSL-510 tunable diode probe laser, swept over a wavelength range of 1520–1580 nm. The input optical power at the on-chip grating couplers was maintained at 15.4 μW after accounting for a coupling efficiency of 1.54%. A representative optical transmission spectrum of a racetrack resonator is presented in Fig. 2(a), where the experimental data are indicated by black circles and the corresponding Lorentzian fit (Eq. (3)) is represented by the orange curve. The fitting process yielded τ, αrt, λres, and [missing symbol] values of 0.974, 0.994, 1547.79 nm, and 14.03 nm, respectively. The point derivative (dT/dλ), illustrated in red, indicates a maximum slope of 450.84 mV/nm and a linear range of 0.06 nm, defined by the vertical dashed lines in the figure.

Likewise, Fig. 2(b) illustrates the optical resonance spectrum of an MZI-racetrack device, with the experimental measurements represented by blue circles and the theoretical fit based on Eq. (2) shown in orange. The fitting parameters b, dneff/dλ, λres, Larm, ng, τ, and αrt were determined to be 0.966, 1.96×10^{-5} nm^{-1}, 1535.26 nm, 33.039 μm, 3.444, 0.976, and 0.996, respectively. The corresponding point derivative (dT/dλ), shown in red, exhibits a maximum slope of 508.88 mV/nm and a linear range of 0.13 nm.

Both devices presented in Fig. 2 were designed with identical coupling conditions. A direct comparison highlights the primary advantage of the ring-loaded MZI, namely, an approximately twofold enhancement in the linear range while maintaining a comparable maximum cavity slope. The theoretical fitting of the transmission spectra obtained from all 24 racetrack-loaded MZIs and 24 reference racetracks revealed closely matched transmission coefficients, with a maximum discrepancy of only 1.3%. The fitted αrt and τ values for individual devices are provided in [7].

The maximum slope point of the resonance determines the sensitivity limit of the photonic circuit to nanomechanical vibrations [5] and, consequently, represents the optimal operating point for the detection laser. When the optomechanical coupling, $G = \partial x \omega res$, is sufficiently strong, shifts in the cavity resonant frequency ωres caused by large-amplitude mechanical vibrations in x, relative to the detection laser setpoint ωl, result in transient movement of the operating point along the transmission spectrum [7,11,12]. If the cavity slope at the operating point changes sign during an oscillation cycle, the mechanical response becomes significantly nonlinear.

To quantify this behavior, we define an empirical linear range as twice the wavelength interval between the cavity minimum (where the slope is zero) and the maximum slope point, with the range centered at the maximum slope point, as illustrated by the dashed lines in Fig. 2(a). Similarly, the Fano linear range is defined as twice the wavelength interval between the zero-slope point and the maximum-slope point, as depicted in Fig. 2(b). The primary objective of this study was to

enhance the linear transduction range of the cavity rather than the range of linear proportionality between the mechanical amplitude and the overall signal power. The amplitude-to-power conversion is governed by the cavity slope and measurement gain.

The maximum slope and linear range measured across all 48 devices are presented in Fig. 3, where the racetrack resonators are represented by red stars and the MZI-racetrack devices by blue dots. The average slope and linear range values, summarized using box plots, demonstrate that the MZI devices provide a 2–3-fold enhancement in linear range under overcoupled conditions, a 1.8-fold enhancement near critical coupling, and a 3.2-fold enhancement under undercoupled conditions. Furthermore, the photonic transduction responsivity (slope) of the MZI-racetrack devices is higher by factors ranging from 1.7 to 3.5 under overcoupled conditions, while remaining comparable to that of the conventional racetrack resonators under critically coupled and undercoupled conditions.

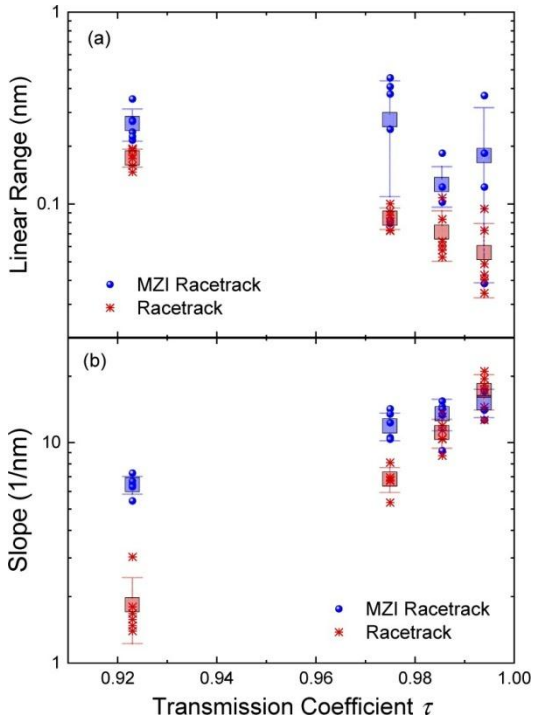

Fig. 3. The linear range (in nm) (a) and the slope (in 1/nm) (b) are plotted for racetrack-type ring resonators (red stars) and Mach-Zehnder interferometers incorporating such resonators (blue circles), as a function of the adjusted mean transmission coefficient τ (0.923, 0.975, 0.986, and 0.994). The mean linear range (a) and the mean slope (b), for each coupling condition and each circuit architecture, are presented using box plots accompanied by standard deviation bars.

Mechanical characterization

The enhancement in linear transduction performance provided by the MZI circuit was experimentally validated by evaluating the mechanical linear range during the readout of side-coupled flexural-mode cantilevers [6]. For this investigation, racetrack-loaded MZIs and reference racetrack resonators were integrated with 3.5 μm-long cantilevers. These cantilevers exhibited fundamental eigenfrequencies of 23.5 MHz, modal masses of 80.4 fg, quality factors of 5000 (at 10^{-4} Torr and 298 K), and cantilever-to-racetrack gaps of 160 nm (G = 0.6 rad GHz/nm) [7]. For each device, the probe laser incident on the input grating coupler was tuned to the maximum transduction point (peak slope) of its previously characterized optical resonance.

The thermomechanical (TM) noise of the cantilevers was recorded under vacuum conditions (10^{-4} Torr) using a Zurich Instruments ultrahigh-frequency (UHF) lock-in amplifier (LIA) controlled through LabONE software, following the procedure described in [7], to calibrate the mechanical amplitude. The transduction responsivity (V/m) was obtained by fitting the TM power spectral density with a Lorentzian function, as described in [27]. The mechanical linear range can be directly quantified by identifying the fundamental (1f) cantilever amplitude at which the second (2f) harmonic signal initially appears [13]. The emergence of higher-order harmonics is considered an indication of the onset of nonlinear behaviour. Specifically, the 1f harmonic signal originates from the slope of the optical transmission curve sampled during the oscillation cycle, whereas the 2f harmonic component indicates the presence of non-zero curvature in the optical transmission response. Accordingly, the 1f and 2f signals were monitored at progressively increasing actuation levels to determine the critical amplitude at which nonlinear behaviour begins.

Mechanical actuation was achieved using a 1.0 mWPhotonetics TUNICS-BT pump laser with a coupling efficiency of 1.54%, tuned to the optical resonant wavelength corresponding to the maximum driven mechanical signal power. Positioning the pump laser at the steepest-slope point of the racetrack-MZI Fano response and at the transmission minimum of the racetrack Lorentzian response also helps prevent unintended self-oscillation (optomechanical damping rate [11], Γopt = 0), while enabling maximum resonant power enhancement for mechanical actuation [7]. The maximum optical damping rate induced by the 15.4 μW probe light in the bus waveguide of our Doppler-regime device was Γopt = 1 Hz.

The pump laser was tuned to an optical resonance different from the one monitored by the probe laser. This arrangement allowed a fibre-coupled optical band-pass filter (with a bandwidth of 0.25 nm), positioned at the output, to selectively transmit only the probe light to the photodiode. Before coupling the laser power into the chip, it was routed through a Lucent Electro-Optic Modulator (EOM) to generate an AC voltage modulation for in-phase mechanical actuation. The voltage amplitudes were supplied from the LIA to the EOM. For each device, the driven 1f and 2f signals were experimentally fitted using Lorentzian functions to determine their peak amplitudes (in volts) as a function of the AC drive voltage. The driven 1f amplitudes were subsequently converted into metres using the transduction responsivity (V/m) [27], thereby compensating for minor variations in actuation power and enabling a direct comparison between devices.

Figures 4(a) and 4(b) illustrate the 2f signal as a function of the fundamental amplitude for the racetrack resonators (red stars) and MZI-racetrack devices (blue circles) under (a) critically coupled (τ = 0.986) and (b) undercoupled (τ = 0.994) conditions, respectively. Under critically coupled conditions, the conventional racetrack resonator exhibited the onset of the 2f signal at a 1f amplitude of 0.3 nm, whereas the MZI-racetrack device showed its onset at 0.8 nm. This result demonstrates a minimum improvement of approximately 2.7× in the mechanical linear range. Moreover, the 2f signal of the MZI-racetrack device did not reach the 9 μV amplitude observed in the conventional racetrack resonator until the 1f amplitude increased to 1.2 nm, suggesting a linear range enhancement approaching 4×.

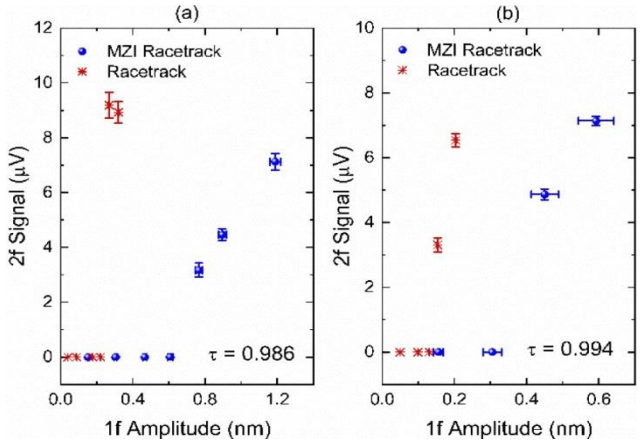

Fig. 4. The 2f harmonic signal (μV) is plotted vs. the fundamental (1f) mechanical amplitude (nm) for the racetrack resonators (red stars) and the MZI racetracks (blue circles). Results are depicted for devices that are (a) critically coupled, τ = 0.986, and (b) undercoupled, τ = 0.994.

The mechanical linear range generally improves as the devices transition towards stronger overcoupling; however, this enhancement comes at the expense of transduction sensitivity and optical power enhancement. The optical power enhancement reaches its maximum near the critical coupling condition [7]. Limitations associated with pump power can be addressed by increasing the EOM-driven amplitude or optomechanical coupling. However, such increases may introduce transduction nonlinearities unless they are accompanied by corresponding improvements in cavity linewidth and overall dynamic range, which are provided by the proposed MZI-racetrack architecture. As demonstrated in Figs. 2 and 3, the MZI device with τ = 0.976 provides an effective balance between linear range and transduction sensitivity while also offering more favourable optical power enhancement for pumping applications [7].

Furthermore, the racetrack-loaded MZI architecture demonstrates superior performance compared with the conventional standalone racetrack design for mass-sensing applications. Mass sensitivity is proportional to the mechanical eigenfrequency shift $\delta\Omega 0/\Omega 0$ and is determined by the ratio of adriven to anoise, expressed through the signal-to-noise ratio (SNR) [1]. Here, SNR represents the signal-to-noise ratio, adriven denotes the amplitude of the 1f signal immediately before the onset of 2f readout nonlinearity, and anoise represents the peak amplitude of the thermomechanical (TM) noise.

For instance, under the coupling condition τ = 0.986, the MZI-racetrack device exhibits an adriven of 0.61 nm and an anoise of 87.4 pm/Hz1/2. In comparison, the conventional racetrack resonator exhibits an adriven of 0.22 nm and an anoise of 87.6 pm/Hz1/2. Based on a 1 Hz measurement bandwidth, the corresponding SNR values for the racetrack-loaded MZI and standalone racetrack devices are 698 and 251, respectively. These results demonstrate that the racetrack-loaded MZI architecture improves the mechanical eigenfrequency shift sensitivity ($\delta\Omega 0/\Omega 0$) by approximately 2.8× compared with the conventional racetrack design.

CONCLUSION

To address readout nonlinearities in racetrack-based optomechanical systems, we designed, fabricated, and experimentally investigated silicon-on-insulator (SOI) racetrack-loaded Mach–Zehnder interferometers (MZIs), comparing their performance with conventional racetrack resonators of identical dimensions. The proposed design consists of an all-pass racetrack resonator coupled to one MZI arm, while the reference arm introduces a phase shift of π/2 at 1550 nm.

Experimental results demonstrate significant improvements in optical linear range, with enhancement factors of 2–3x under overcoupled conditions, 1.8x near critical coupling, and 3.2x under undercoupled conditions. Transduction sensitivity also improves by 1.7x–3.5x in the overcoupled regime. Furthermore, mechanical measurements reveal a 3–4x enhancement in linear range and a 2.8x improvement in frequency-shift sensitivity compared with conventional racetrack resonators.

These findings establish the racetrack-loaded MZI as a promising architecture for high-dynamic-range nanomechanical sensing, including mass, temperature, and biochemical applications. Additionally, its phase-sensitive integrated configuration offers potential for on-chip homodyne detection. Future improvements, including adjustable optical splitting ratios (50:50 to 90:10) and balanced homodyne detection using a 2 × 2 output coupler, could further enhance detection sensitivity and signal-to-noise ratio [29].

REFERENCES

1. D. Sinha, D. De, A. Ayaz, Performance, and stability analysis of curcumin dye as a photo sensitizer used in nanostructured ZnO based DSSC, Spectrochim. Acta A. 193 (2018) 467–474. S. K. Roy, V. T. K. Sauer, J. N. Westwood-Bachman, A. Venkatasubramanian, and W. K. Hiebert, "Improving mechanical sensor performance through larger damping," Science 360(6394), eaar5220 (2018).

2. Venkatasubramanian, V. T. K. Sauer, S. K. Roy, M. Xia, D. S. Wishart, and W. K. Hiebert, "Nano-Optomechanical Systems for Gas Chromatography," Nano Lett. 16(11), 6975–6981 (2016).

3. T. P. Purdy, K. E. Grutter, K. Srinivasan, and J. M. Taylor, "Quantum correlations from a room-temperature optomechanical cavity," Science 356(6344), 1265–1268 (2017).

4. Yu, Y. Zhang, X. Zhang, K. Wang, C. Yao, P. Yuan, and Y. Guan, "Nested fiber ring resonator enhanced Mach-Zehnder interferometer for temperature sensing," Appl. Opt. 51(36), 8873–8876 (2012).

5. V. T. K. Sauer, Z. Diao, M. R. Freeman, and W. K. Hiebert, "Optical racetrack resonator transduction of nanomechanical cantilevers," Nanotechnology 25(5), 055202 (2014).

6. V. T. K. Sauer, Z. Diao, M. R. Freeman, and W. K. Hiebert, "Nanophotonic detection of side-coupled nanomechanical cantilevers," Appl. Phys. Lett. 100(26), 261102 (2012).

7. J. Bachman, "Improving the performance of nano-optomechanical systems for use as mass sensors," Ph. D. Thesis, University of Alberta, (2019).

8. S. Xiao, M. H. Khan, H. Shen, and M. Qi, "Compact silicon microring resonators with ultra-low propagation loss in the C band," Opt. Express 15(22), 14467–14475 (2007).

9. P. Cai, J. H. Lu, C. C. Chen, C. C. Lee, C. E. Lin, and T. J. Yen, "High Q-factor microring resonator wrapped by the curved waveguide," Sci. Rep. 5(1), 10078 (2015).

10. Gavartin, P. Verlot, and T. J. Kippenberg, "Stabilization of a linear nanomechanical oscillator to its thermodynamic limit," Nat. Commun. 4(1), 2860 (2013).

11. M. P. Maksymowych, J. N. Westwood-Bachman, A. Venkatasubramanian, and W. K. Hiebert, "Optomechanical spring enhanced mass sensing," Appl. Phys. Lett. 115(10), 101103 (2019).

12. M. Poot, K. Y. Fong, M. Bagheri, W. H. P. Pernice, and H. X. Tang, "Backaction limits on self-sustained optomechanical oscillations," Phys. Rev. A: At., Mol., Opt. Phys. 86(5), 053826 (2012).

13. H. Rokhsari, T. J. Kippenberg, T. Carmon, and K. J. Vahala, "Radiation-pressure-driven micro-mechanical oscillator," Opt. Express 13(14), 5293–5301 (2005).

14. J. Lee, Z. Wang, K. He, R. Yang, J. Shan, and P. X. L. Feng, "Electrically tunable single- and few-layer MoS2 nanoelectromechanical systems with broad dynamic range," Sci. Adv. 4(3), eaao6653 (2018).

15. N. Kacem, J. Arcamone, F. Perez-Murano, and S. Hentz, "Dynamic range enhancement of nonlinear nanomechanical resonant cantilevers for highly sensitive NEMS gas/mass sensor applications," J. Micromech. Microeng. 20(4), 045023 (2010).

16. L. G. Villanueva, E. Kenig, R. B. Karabalin, M. H. Matheny, R. Lifshitz, M. C. Cross, and M. L. Roukes, "Surpassing fundamental limits of

oscillators using nonlinear resonators," Phys. Rev. Lett. 110(17), 177208 (2013).

17. J. Melcher, J. Stirling, F. G. Cervantes, J. R. Pratt, and G. A. Shaw, "A self-calibrating optomechanical force sensor with femtonewton resolution," Appl. Phys. Lett. 105(23), 233109 (2014).

18. Y.Lu, J.Yao,X.Li, and P.Wang, "Tunable as ymmetricalFanoresonancebistabilityinamicrocavity -resonator-coupled Mach Zehnder interfero meter," Opt. Lett.30(22), 3069–3071 (2005).

19. V. Van, W. N. Herman, and P. T. Ho, "Linearized microring-loaded Mach-Zehnder modulator with RF gain," J.Lightwave Technol.24(4), 1850–1854 (2006).

20. S.Darmawan,Y.M.Landobasa,P.Dumon,R.Baets,and M.K.Chin,"Nested-RingMach–Zehnder Interfero meter in Silicon-on-Insulator," IEEE Photon. Technol. Lett.20(1), 9–11 (2008).

21. J.A.Cox,A.L.Lentine,D.C.Trotter,andA.L.Starbuck," Controlofintegratedmicro-resonator wave length via balanced homodyne locking," Opt. Express22(9), 11279–11289 (2014).

22. F. Raffaelli, G. Ferranti, D. H. Mahler, P. Sibson, J. E. Kennard, A. Santamato, G. Sinclair, D. Bonneau, M. G.Thompson, and J. C. F. Matthews, "A homodyne detector integrated onto a photonic chip for measuring quantumstates and generating random numbers," Quantum Sci. Technol.3(2), 025003 (2018).

23. A.H.Safavi-Naeini, S.Gröblacher, J.T.Hill, J.Chan, M.Aspelmeyer, and O.Painter, "Squeezed light from a silicon micro mechanical resonator," Nature500(7461), 185–189 (2013).

24. J.N.Westwood-Bachman, Z.Diao, V.T.K.Sauer, D.Bachman, and W.K.Hiebert, "Even nano mechanical modes transduced by integrated photonics," Appl. Phys. Lett.108(6), 061103 (2016).

25. V.Van, Optical Micro ring Resonators: Theory, Techniques, and Applications (CRC,2016).

26. V. T. K. Sauer, Z. Diao, and M. R. Freeman, "Confocal Scanner for Highly Sensitive Photonic Transduction of Nano mechanical Resonators," Appl. Phys. Express6(6), 065202 (2013).

27. M.Li,H.X.Tang, and M.L.Roukes,"Ultra-sensitive NEMS-based can til evers for sensing, scanned probe and very high-frequency applications," Nat. Nanotechnol.2(2), 114–120 (2007).

28. M.Bagheri, M.Poot, M.Li,W.P.H.Pernice, and H.X.Tang, "Dynamic manipulation of nano mechanical resonatorsin the high-amplitude regime and non-volatile mechanical memory operation," Nat. Nano technol.6(11), 726–732(2011).

29. A. Schliesser, R. Rivière, G. Anetsberger, O. Arcizet, and T. J. Kippenberg, "Resolved-sideband cooling of a micro mechanical oscillator," Nat. Phys.4(5), 415–419 (2008).

BIOGRAPHIES



Surabhi Gupta

Assistant Prof., Department of Applied Sciences and Humanities (Engineering Physics), VSGOI, Unnao, AKTU, U.P India